Lightning Currents on Fastening Assemblies of Aircraft Fuel Tank - Part I: Uncertainties Assesment with Statistical Approach

Paul Monferran, Christophe Guiffaut, Alain Reineix, Fustin Fabian, Fabrice Tristant

Lightning Currents on Fastening Assemblies of an Aircraft Fuel Tank, Part I: Uncertainties Assessment with Statistical Approach

P. Monferran, C. Guiffaut, *Member, IEEE,* A. Reineix, *Member, IEEE*, F. Fustin and F. Tristant

Abstract **This paper proposes a statistical approach able to assess the fastening resistances uncertainties in aircraft assemblies. This method relies on the use of the maximum likelihood estimation method, several statistical tests and/or statistical criteria. Using the Dassault-Aviation measurement database, distribution laws are established in order to characterize uncertainties in the lightning impact on the fasteners. A simple FDTD fastener model is proposed with a wire and a resistance. This generic model can represent any fasteners. The statistical model established from the fastener resistances state after a lightning shot is used to define the stochastic distribution values in the fastener electric model. This model is added to a 3D FDTD parallelepiped generic fuel tank model. In this article, we compare the current distributions between a composite and metallic fuel tank. The results highlight not only the model uncertainties effects on the statistical approach but also the fuel tank material choice impact.**

Index Terms**—Statistical method, finite-difference time-domain (FDTD) modelling, fastener modeling, lightning effects, fuel tank aircraft, composite material.**

I. Introduction

ON average, a lightning strikes an airliner once per year [1]. The aircraft zoning defines the zones in interaction with lightning attachment. In these zones, the electric field (E-field) is extremely high [2]. The European Aviation Safety Agency (EASA) and the Federal Aviation Agency (FAA) define the aircraft lightning standard. For both agencies, this standard is attuned by the European Organization for Civil Aviation of Automotive Engineers (EUROCAE) and the Society of Automotive Engineers (SAE) in the document ED-91 [3]. According to the aircraft zoning, few hundred thousand fasteners are located in the sweeping zone on wing fuel tank [2]. They constitute ideal points for the lightning attachment [4]. When a lightning attachment occurs on an aircraft, a high current flows in fasteners involving a high current density in an immediate neighborhood. Furthermore, fasteners are generally the only way to drive the parasitic current in the aircraft structure due to the anticorrosive paint recovering all metallic elements. The high current which flows in fasteners may generate sparking and outgazing effects [5]-[7]. These effects are due to the temperature rising, pressure and voltage [7]-[10].

The electromagnetic (EM) phenomena related to lightning constitute important challenges in the aircraft industry. Increasingly, to understand EM phenomena, EM simulations are used [11]-[14]. In Electromagnetic Compatibility (EMC) the lightning indirect effects have been well-studied [11], [12] in comparison with direct effects. However, direct effects are crucial for the airplane certification.

To avoid catastrophic accidents, protections against fastener sparking in fuel tank have been studied [10], [15-17]. The prevalent protection techniques are based on the will to manage the current distribution on the aircraft structure. Sparking effects occurrences are minimized [10], [18] by adding sealant in critical zones, especially where the electric arc occurs and also by introducing a metallic mesh in safe zones. Another protection solution is to confine sparking with an enclosure located around the fastener [19]. These lightning protections are quite efficient but they are not able to give information about the EM effects of lightning on fastener. The understanding of these effects is a recent requirement in the aircraft industry for the airplane lightning certification. Indeed, the aircraft manufacturers have to design new kinds of fasteners for avoiding sparking effects.

The main parameters in the sparking phenomenon are the contact resistances between fasteners and the structure [4]-[5]. These contact resistances have been studied and usually estimated around few mΩ [4], [6], [7]. However, there is no method to characterize them. Furthermore, for the same kind of fastener, the contact resistances may be more sensitive from one fastener to another. The important challenge for the EMC airplane certification is the fastener modeling and the contact resistances uncertainties considering. In order to ensure this, the application of a statistical model on the parameters of a fastener model is required. We assume that the work presented in this article is intended for the aeronautical field. Nevertheless, the proposed process for the uncertainty model establishment is general. This process can be used to build an uncertainty model from any data which represent the variability of a definite parameter. To that extent, the uncertainty assessment proposed method is attractive in several EMC applications. That is even more true of small samples which make the study difficult.

The writing of this paper was supported by the XLIM Laboratory.

P. Monferran, C. Guiffaut and A. Reineix are with Xlim laboratory, 123 avenue Albert Thomas, 87000 Limoges, France (phone: +33-5-55-45-77-39; fax: +33-5-55-45-77-66; e-mail : paul.monferran@xlim.fr, christophe.guiffaut@xlim.fr and alain.reineix@xlim.fr)

F. Fustin and F. Tristant are with Dassault Aviation Company, 78 Quai Marcel Dassault, 92552 Saint-Cloud, France (e-mail: fabian.fustin@dassault-aviation.com and fabrice.tristant@dassault-aviation.com).

The aim of this article is to propose a practical approach in order to build a statistical model taking into account the uncertainties of the contact resistances from a measurement database. We apply a coherent statistical model on the parameters of a fastener model. Then, they are both integrated in metal and composite fuel tanks modelling. Interaction between fastener uncertainties and the material fuel tank is investigated on the current responses in assembly lines. This interaction is currently one of the most discussed question by the EMC community of the aeronautical field [4], [20], [21].

In the literature very few fasteners models were considered in full-wave computation. Approaches dealt with a very thin mesh representation [7], a wire approach [22] or whether a circuit approach [16]. For all these models one of the main issues is the difficulty to estimate the uncertainties of their parameters and in particular the contact resistances. The fastener model proposed in this paper is a simple resistive model. Each fastener is represented by a contact resistance with a distributed value obtained from a statistical law. Statistical analyses are based on several measurement campaigns made by Dassault-Aviation in the past taking into account equivalent resistance measurements.

In this paper, we propose a statistical fitting method from these measurements data base. Hence the empirical probability distribution is fitted by theoretical laws. We introduce a required preliminary step for the unimodality verification of our data using the Hartigan test [23]. Then, another step is presented for the choice of theoretical laws using in particular the Cullen and Frey graph [24] with a bootstrap procedure [25]. The fitting method is based on the use of maximum likelihood estimation (MLE) [26], [27] followed by goodness-of-fit plots [28] and statistical tests [29], [30] or goodness-of-fit criteria [31]. The probability laws of resistance values supplement our fastener model and are used to analyze the fastener influence in a complex assembly as a fuel tank structure. Our fastener model and the current distribution calculation of one fastening assembly on the fuel tank structure are made using the Finite Difference Time Domain (FDTD) method via our laboratory made FDTD software (TEMSI-FD [32]).

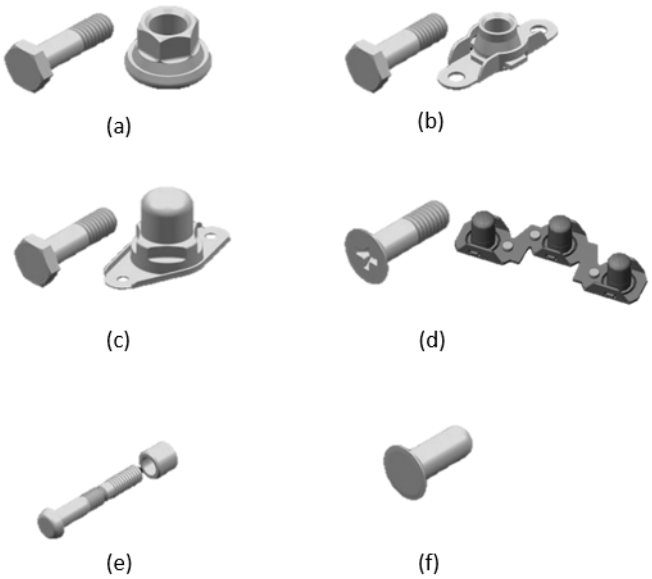

Fig. 1. Illustrations of the different types of fasteners; (a) Hexagonal screw with RH nut (RH), (b) Floating Leak proof nuts on floating nut plate (FLP), (c) Leak proof nuts (LP), (d) Countersunk screw with floating nut plate (FC), (e) MGPL-C rivet (MGPLC), (f) Aluminum rivet (R).

First, the experimental database analysis is introduced in section II presenting the resistance measurements, the statistical trend and the statistical fitting method is detailed with its application. In particular, the chosen statistical approach is justified according to the required hypotheses made on our data. Then, applying the statistical results on our fastener model, a stochastic study about the EM behavior of one fuel tank fastening assembly is carried out in section III.

II. Experimental Database Analysis

A. Measured Samples

The aircraft Companies use various fasteners types in their fastening assemblies. Some of them are represented in Fig. 1. In the past, one hundred samples have been built accounting for various fastening assemblies, each of them is two metallic assemblies screwed by two fasteners. Fig. 2 shows one sample with float nuts with its dimensions. Any sample is designed with two different types of fasteners. However, voluntarily defaults are introduced in some fasteners in order to see their effects compared to nominal case. Finally, database is constituted of 7 kinds of defaults:

- without failures,
- with over-diameter failure,
- with torque failure,
- with sealant failure,
- without paint,
- without sealant and over-diameter failure,
- without sealant and torque failure.

More details about each failure can be found in [33]. In the following, only the measurement between Ref1 and Ref2 (Fig. 2) is taken into account. These resistance measurements are performed using the microhmmeter OM16 [34]. On each sample, one measurement is made before lightning injection and another after lightning injection. Fig. 3 illustrates the trend of resistance values before and after lightning injection for different fasteners presented in Fig. 1 without defaults. Taking

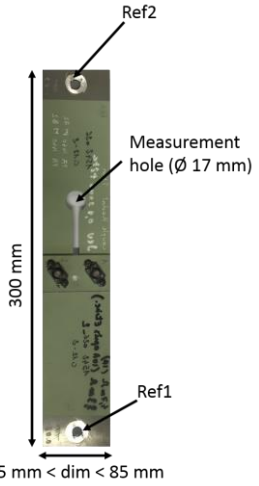

Fig. 2. Picture of the sample with float nuts.

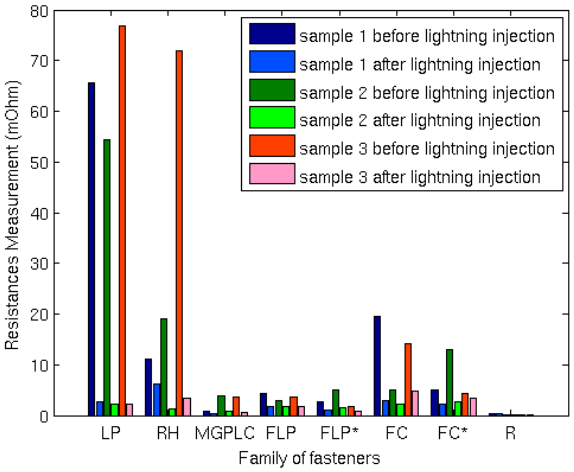

Fig. 3. Database fragment illustrating DC measurement of sample without default for several fastener types before and after lightning injection (* means that the diameter of the screw is different). For each type, three samples are measured.

into account the full database, we note that usually the lightning injection modifies the resistances by decreasing their values (around -10 dB which represents a factor 3). Nevertheless, for fasteners with really low values before lightning injection (as aluminum rivet), the impact is really weak. As a consequence the aluminum rivets samples are not studied. Moreover, dispersion of data before lightning injection is high even for same type of fasteners used (around 8 dB). This trend is effectively verifiable in the other samples of our database.

B. Statistical fitting method

In this section, we take an interest in the search of statistical laws which could represent uncertainty behavior of the resistances values. In particular, the lightning injection effect and the distribution of the resistances values after lightning injection are studied. The proposed method is general and therefore it can be applied for any data provided that some hypotheses about them. Three main hypotheses must be made for our data: 1) the data are continuous, 2) independent and 3) the process required the use of non-parametric tests. Indeed in our case, all the studied data come from contact resistances measurements of fasteners and are always continuous. Following this hypothesis, the Chi-square test (χ^2), usually used for discrete data, does not be used. Moreover, we suppose the data independence since each measurement and each measured sample are independent from one another. Therefore, correlation analysis must be avoided. Furthermore, we assume that parametric assumptions cannot be made especially because of the impossibility of supposing the data normality distribution and the equal variances. In this instance, only non-parametric tests are used.

The general process is presented in Fig. 4. This flowchart details the process to fit as much as possible empirical data with a theoretical law. This method based on the MLE method, several statistical tests and goodness-of-fit criteria follows five steps as illustrated in Fig. 4:

1. Verify unimodality of the empirical probability distribution function (PDF) and cumulative distribution function (CDF).

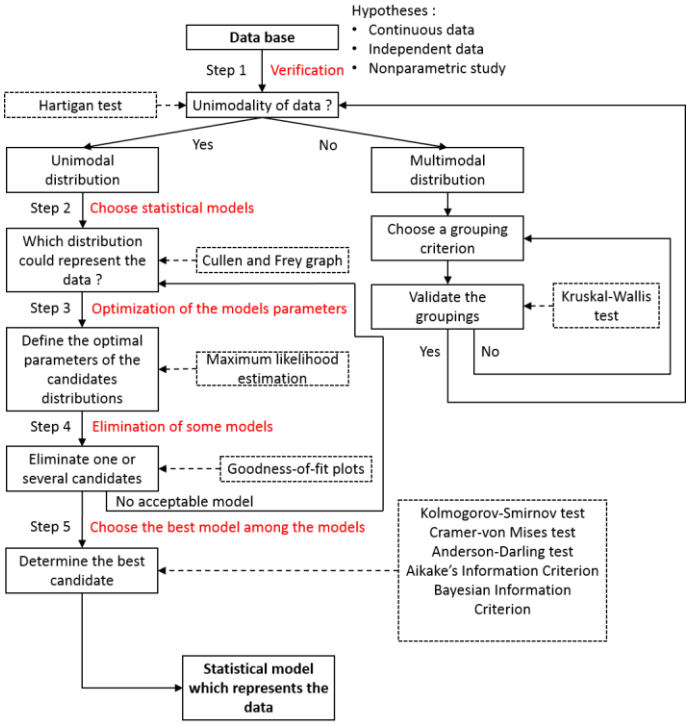

Fig. 4. Flowchart of the statistical fitting method.

2. Choose candidate distributions according to empirical distributions and the skewness and kurtosis.
3. Use maximum likelihood estimation to fit the distribution.
4. Choose the best candidates using four classical goodness-of-fit plots (PDF, CDF, probability-probability plot called P-P plot, and quantile-quantile plot called Q-Q plot).
5. Determine the best candidate with statistical tests and goodness-of-fit criteria.

Step 1 is mandatory in most statistical analyses. Indeed, when we have a sample database, it is required to verify if the samples may form a uniform group from a statistical point of view. The Hartigan test [23] allows us to evaluate the unimodality of the empirical distributions with a maximum error of α%. In most of case, we choose 95% confidence degree corresponding to $\alpha = 0.05$. We choose to use the Hartigan test because it is a general non-parametric test which can be applied for small samples without any assumption about the normal mixture as for the proposed tests in [35] and [36].

Furthermore, if the data distribution is not unimodal, a grouping study is required. We propose in this case to split the data in several samples populations according to an intrinsic criterion of the data. Typically, a family fastener grouping or a default type grouping can be made in our case. Then, statistical criteria, as for instance the mean and the variance, might be used to group together several populations. In order to validate these groupings, we propose to use the Kruskal-Wallis test [37]. This non-parametric test is useful for small samples populations with unknown distributions. Moreover, it can be applied for many groups in contrast to the Wilcoxon signed-rank test [38] for instance. Finally, if the grouping is validated, steps 1 to 5 can be applied with these new data. Otherwise, a new intrinsic criterion must be defined until the grouping validation.

The following steps are dedicated to the search of a statistical model which represents in a good way the statistical data behavior. The proposed approach might be slightly modified according to the data behavior. We detail here each step and we give some alternatives specifically for the parameters' estimation.

The aim of the step 2 is to choose statistical models that represent data in the better way. We use first the graphical appearance of the PDF in order to choose some candidates. Moreover, the Cullen and Frey graph [24] might be helpful to choose candidates. It uses the third and fourth order moments depicted by skewness-kurtosis plots. For some distributions (normal, uniform, logistic, exponential), only one value for the skewness and the kurtosis is possible. Thus, the distribution is represented by a single point on the plot and the law is symmetric. For other distributions, areas of possible values are represented, consisting in lines (as for the gamma and lognormal distributions), or larger areas (as for the beta distribution). Nevertheless, the high variance of these higher moments involves that the Cullen and Frey graph is only an indication for the choice of candidates. A nonparametric bootstrap procedure [25] might be performed in order to improve the analysis. The bootstrap procedure is based on random sampling with replacement from the original data set. The bootstrapping principle is to take the original data set and sampling from it to form a new sample called bootstrap sample. Repeating this process a large number of time, statistic, estimators or statistical moments can be computed and their variations can be estimated from the bootstrap sample. The size of the bootstrap sample and the number of bootstrap samples can be found in [25] according to the used bootstrap method. Thus, in our case, 1000 others kurtosis-skewness values are computed with the 1000 bootstrap samples with the same size of the original data set.

The step 3 lies on an optimization of the parameters of our candidate distributions by the MLE [26], [27]. Although this method is well-known, the principle is reminded below. We define θ as parameter of distribution, x_i a value or measure of variable X and f the density function. The aim is to maximize the likelihood function defined as

$$L(\theta) = \prod_{i}^{n} f(x_i | \theta), \quad (1)$$

By determining θ such as:

$$\frac{\partial L(\theta)}{\partial \theta} = 0 , \quad (2)$$

to have an optimum and to be sure that is a maximum:

$$\frac{\partial^2 L(\theta)}{\partial \theta^2} < 0. \quad (3)$$

Furthermore, it is well known that the MLE method is sensitive with outliers. Usually, these ones can be easily removed from the database in the case of small samples. Nevertheless, for a large number of samples, the removing might be difficult. Consequently, alternative methods can be used to enhance the parameter estimation. Typically, the moment matching estimation (MME) is frequently used because of its reliability [39]. The MME can be considered as a more cautious estimation than the MLE. Nevertheless, the MME presents a high sensitivity to outliers as for the MLE method. Furthermore, the maximum goodness-of-fit estimation (MGE) method provides a straightforward alternative to using the MLE particularly in order to give more weight to the tails [40].

In step 4, we compare the four classical goodness-of-fit plots (PDF, CDF, P-P plot, Q-Q plot) using parameter of distribution computed in step 3. PDF plots and CDF plots may be considered as the basic goodness-of-fit plots. In the other hand, Q-Q plots represent the distribution tails and P-P plot the distribution center. According to the statistical study in this paper, we choose to have more details on the general distribution rather than for the extreme values. With these indications, the best candidates might be chosen even if the choice is not always easy to make because of the accuracy of these plots. At least, one candidate can be usually removed.

In order to improve our graphical feelings, each theoretical distribution is submitted to statistical tests and goodness-of-fit criteria in the step 5. The Kolmogorov-Smirnov (KS), Cramer-von Mises (CvM) and Anderson-Darling (AD) tests are used in this paper. These tests are performed using empirical CDF data and candidate CDF data. Furthermore, these tests require conditions about data number (usually more than 30 are needed) [29], [30] and kind of distributions (CvM and AD limited to some distributions as exponential, Weibull, Gamma or Cauchy distributions) [41]. Nevertheless, the tests can be computed and might be a useful indicator (the weaker result, the better distribution). Moreover, two goodness-of-fit criteria, the Aikake′s Information Criterion (AIC) and Bayesian Information Criterion (BIC), are used in order to compare the candidate distributions together [31]. They are both based on the log-likelihood [31] requiring the use of the MLE method as fitting method. Nevertheless, AIC and BIC can be computed with the MME or MGE applying a post-treatment to the fitting curve determined. As for the computed results of tests, the more the criteria is weak the better the candidate distribution will be fitted. The aim is to compare together the fitted statistic models. In this way, it is preferable to determine the best model from the proposed ones using the AIC and BIC than the goodness-of-fit tests (KS, CvM and AD).

C. Applications of the statistical method

Our data base consists of 84 measures of resistances made before lightning injection and 84 measures after lightning injection for different kind of fasteners with or without defaults. The measurement of aluminum rivets is not considered as mentioned in section II. This subsection is split in two subsubsections. A first one is devoted to the fasteners state using the measurements after lightning injection. Furthermore, a second one related to the lightning injection effects is performed.

a) On measurements after lightning injection

We note that 96% of measurements after lightning injection (81/84) have resistance values lower than 10 mΩ. Fig. 5 presents the PDF and CDF of these data. At first sight, the distributions seem unimodal. The Hartigan test validates our standpoint with a 95% confidence degree. Fig. 6 presents the Cullen and Frey graph for our data with a bootstrap procedure with 1000 values. According to these graphs (Fig. 5 and Fig.

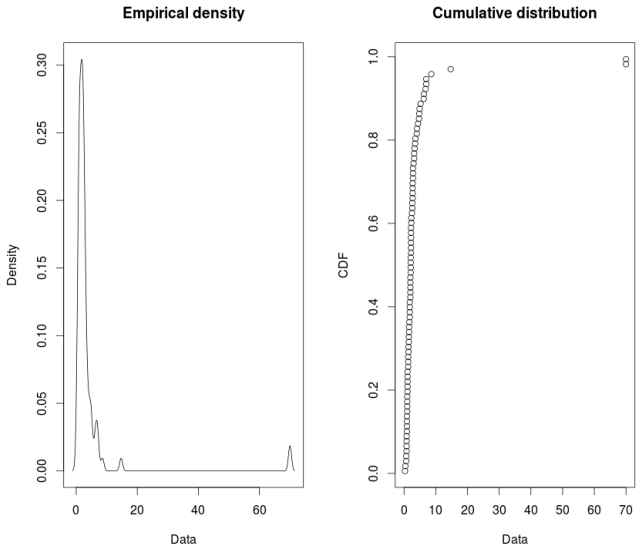

Fig. 5. Empirical probability (left) and cumulative (right) density functions of resistances values after lightning injection.

6), we choose to fit four distributions; Weibull, Lognormal, Loglogistic and Beta.

Then, we apply the MLE method on each theoretical distribution, after that, we compare the goodness-of-fit plots. Fig. 7 presents each of these plots. According to them, the Loglogistic and Lognormal distributions seem to be better than the two others. This step usually allows us to eliminate some candidate distributions. Nevertheless, it is really hard to give the better one with these graphical analyses. Hence, we use the statistical tests and the goodness-of-fit criteria presented in the previous subsection in order to quantify our results. The results are presented in Table I. It confirms our previous assumptions about the best distributions. Looking at the results, the lognormal distribution, with $\mu = -1.524$ and $\sigma = 0.665$ as parameter values, is the best to represent the fasteners resistances distribution after lightning injection. Using the other parameters estimation method as the MME and the MGE with a strong weight on the right tail, the deviation between them is sufficiently small (Fig. 8) to disregard any difference between them.

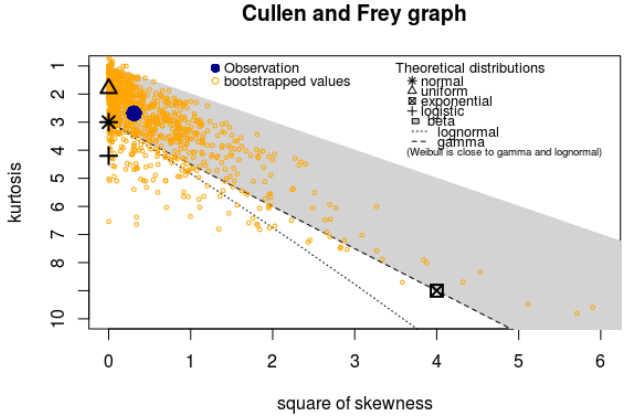

Fig. 6. Cullen and Frey graph analyzing the third and the fourth moments of empirical distribution.

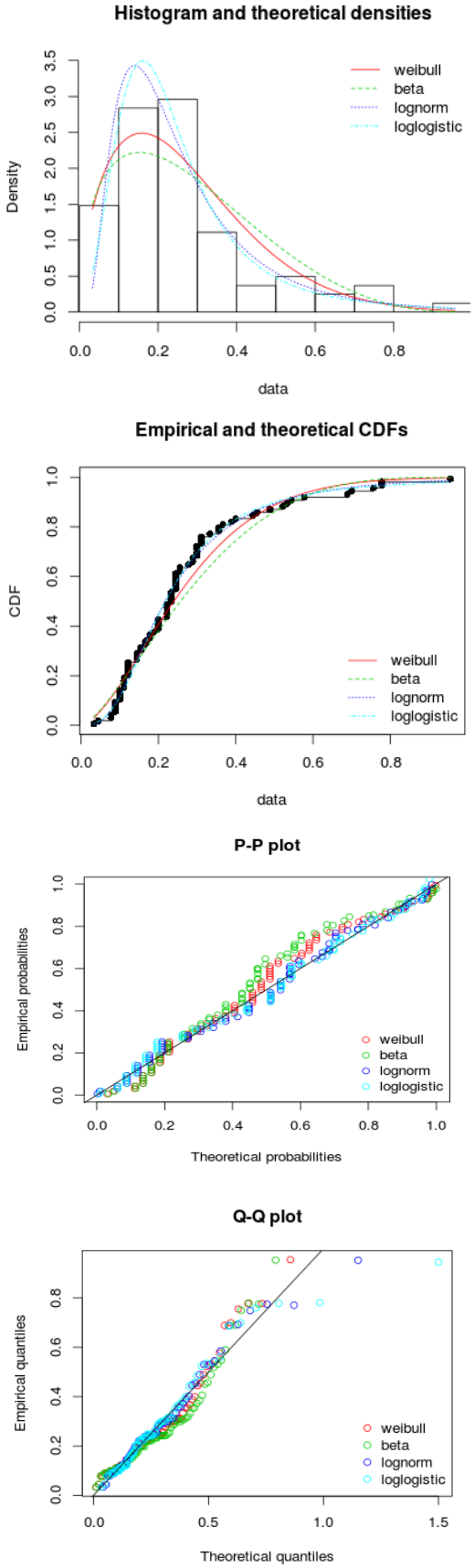

Fig. 7. Four classical goodness-of-fit plots PDF, CDF, P-P plot, Q-Q plot with empirical data (black) and candidate distributions data.

TABLE I
RESULTS OF STATISTICAL TESTS AND GOODNESS-OF-FIT CRITERIA VALUES FOR CANDIDATE DISTRIBUTIONS.

	Weibull	Beta	Lognormal	Loglogistic
KS	0.1187✓	0.1629×	0.07970✓	0.08120✓
AD	0.1990×	0.4220×	0.06194†	0.06238†
CvM	1.2966×	2.3766×	0.38731†	0.40508†
AIC	-69.63	-59.77	-79.06	-77.65
BIC	-64.84	-54.98	-74.27	-72.86

✓ Approved test
× Rejected
† Not computable

b) On lightning injection effect

The aim is to define trends of lightning injection effects in function of sample family or failure modes. 160 measurements data; 80 before lightning injection noted R_{before} and the 80 after noted R_{after}, are studied. First, a random variable has to be defined in order to characterize the lightning injection effect. We defined two normalized variables as a lightning injection effect:

$$\Delta R_{diff} = \frac{1}{80}\left\lceil 20\log\left(\frac{R_{before}}{R_{after}}\right)+40\right\rceil \quad (4)$$

and,

$$R_{diff} = \frac{1}{2}\left\lceil\left(\frac{R_{before}-R_{after}}{R_{before}+R_{after}}\right)+1\right\rceil. \quad (5)$$

Both have the value 0.5 corresponding to the equality between resistances before and after lightning injection. Using (4) we examined the lightning injection effects looking to the division between R_{before} and R_{after} in dB which is equivalent to a relative error in dB when both resistance are close. In the other hand, (5) presents the relative difference between R_{before} and R_{after}. According to Fig. 9, the distributions of both variables seem to be multimodal. Furthermore, the bias due to the choice of each variable is clearly highlighted. The

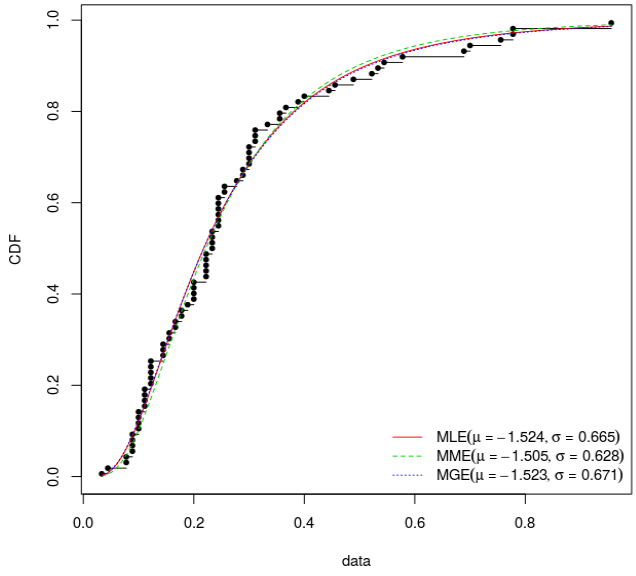

Fig. 8. Comparison between MLE, MME and MGE (weight on right tail) when fitting a lognormal distribution to data from the measurements after lightning injection

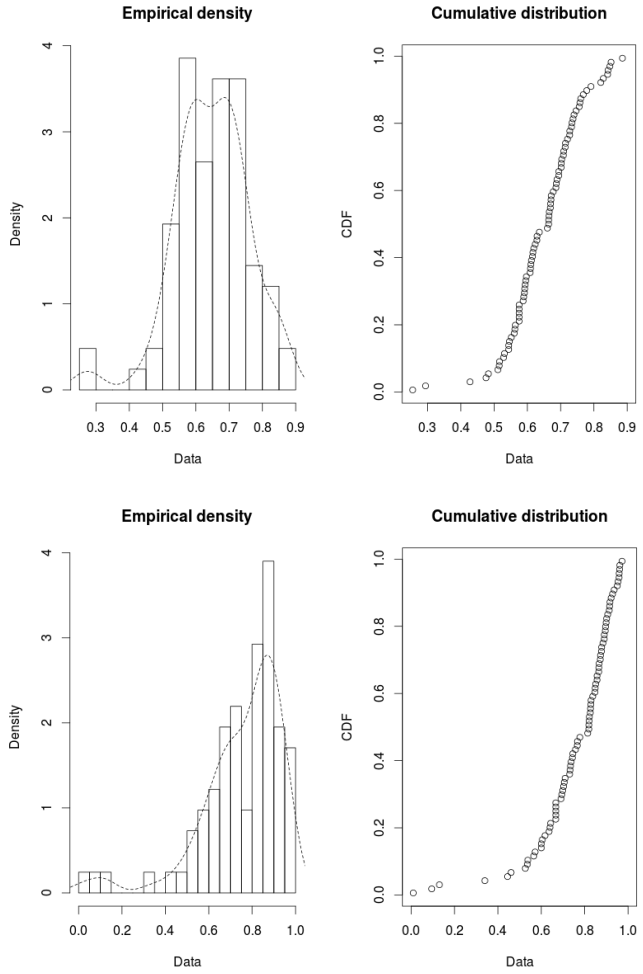

Fig. 9. Empirical PDF (left) and CDF (right) of ΔR_{diff} (top plot) and R_{diff} (bottom plot).

multimodality of each distribution is confirmed by the reject of the Hartigan test. The previous statistical fitting method cannot be used according to the step 1. Unfortunately, the Hartigan test cannot give us the number of distribution modes. In this case, one solution may be to group some data according to physical criteria.

We choose the failure modes as grouping criterion. First and second moments (mean μ and variance σ) are computed as indicator. Table II presents the mean and variance of measurements for each failure mode. Apparently, some failure modes have the same statistical trend whatever the random variable is. From the results, we can define three populations which seem to have similar statistical trend. The first one, noted population 1, is composed by 30 samples using the "without failure" mode, "without paint" failure mode and "without sealant and over-diameter failure" mode. The second one, denoted population 2, is constituted with 38 samples from the "over-diameter" and "torque" failure mode. The last one, noted population 3, has only 12 samples, 6 from "without sealant" failure mode and 6 from "without sealant and torque" failure mode.

In order to validate these groupings, the Kruskal-Wallis non-parametric test is performed. The results of this test indicate that there are insignificant differences between the sub-populations (here failure modes) in the new populations

TABLE II
MEAN AND VARIANCE OF MEASUREMENTS FOR EACH FAILURE MODE.

	ΔR_{diff}		R_{diff}	
	mean	variance	mean	variance
Population 1				
No failure	-12.93	8.70	-0.55	0.25
Without paint	-11.69	7.96	-0.53	0.38
Without sealant and over-diameter	-11.95	7.02	-0.54	0.28
Population 2				
Over-diameter	-9.80	10.59	-0.37	0.50
Torque failure	-9.08	9.14	-0.43	0.38
Population 3				
Without sealant	-15.58	3.33	-0.70	0.09
Without sealant and torque failure	-16.79	3.66	-0.78	0.04

defined below. Therefore, our groupings are validated. Then, the steps 2 to 5 of the statistical fitting method can be performed. The results for each population and each variable are described in Table III. For the sake of brevity, the plots of each result are not presented but we assure that they are all different. The differences between the laws of each population are not surprising; each population has a particular response to the lightning injection. Furthermore, the bias discussed before is highlighted according to the different probability laws established for the population 1 for instance. Indeed, it highlights that the choice of the metric (here ΔR_{diff} or R_{diff}) has an important influence. In our case, for each metric a different lightning shot effect is observed involving as a consequence different probability laws. Moreover, using R_{diff} in the population 2, any probability laws has been fitted the empirical one because of a lack of samples. The accuracy of the results of the population 3 can be discussed for the same reason.

III. FUEL TANK MODELLING RESULTS

A. Fuel Tank and Fastener Modelling

Each fastener is represented with a wire and a resistance corresponding to the resistance measurements done between Ref1 and Ref2 (Fig. 2). This kind of model allows us to represent any kind of fasteners whatever their position thanks to the oblique thin wire formalism in the FDTD method [42]. Moreover, it is easy to implement our fastener model in the fuel tank FDTD modelling. The fuel tank modelling is simplified in a generic form. Fig. 10 depicts the fuel tank FDTD modelling with a zoom on the fastener assembly. Only one fastener assembly is represented. The fuel tank dimensions are 100x50x25 cm^3 (LxWxH). The assembly line is made up of 30 fasteners. Each fastener is placed on an edge of the FDTD grid and two consecutive fasteners are separated by one cell only. The fastening assembly is thus represented as a crown-shaped wire network all around the parallelepiped fuel tank. The fasteners constitute the only way to drive the current from one part (in turquoise) to the other one (also in turquoise) of the fuel tank.

TABLE III
PROBABILITY LAWS FITTED FOR EACH POPULATION AND EACH VARIABLE.

	ΔR_{diff}	R_{diff}
Population 1 (30 samples)	Lognormal	Beta
Population 2 (38 samples)	Weibull	Undetermined
Population 3 (12 samples)	Weibull	Weibull

The lightning frequency band is defined from zero hertz to few megahertz according to the Fourier transform of the A-type waveform [43]. A Gaussian waveform is used rather than an A-type waveform in order to avoid long time simulation. Nevertheless, FDTD simulation at low-frequencies may need a long computation time. As a consequence, we split each simulation into two frequency bands. The first one covers the 100 kHz-1 MHz bandwidth. The second one from 100 Hz to 100 kHz, is computed using a low frequency acceleration technique [44]. Indeed, the mesh step Δ is extremely smaller against the smaller wavelength $\lambda_{\min}$ (here $\Delta = \lambda_{\min} / 6000$). Moreover, long excitation pulses are needed for a low frequency spectrum. Hence, the iteration number is huge and the system response is too long to solve. Therefore, the low frequency acceleration technique allows the computation convergence within a reasonable time. The principle is to increase the vacuum permittivity [44] with a factor α as follows:

$$\varepsilon_0^{new} = \alpha^2 \varepsilon_0 . \quad (6)$$

Thus, the time step constraint of the FDTD method which is capped by the Courant-Friedrichs-Lewy condition (CFL) [45] is released as

$$\Delta t^{new} = \alpha \, \Delta t . \quad (7)$$

This modification does not affect the eddy current calculated with the Maxwell's curl H equation. Nevertheless, displacement current must be insignificant in comparison with conduction current:

$$j \varepsilon_0^{new} \varepsilon_r \omega E << \sigma E . \quad (8)$$

Therefore, the vacuum permittivity modification does not

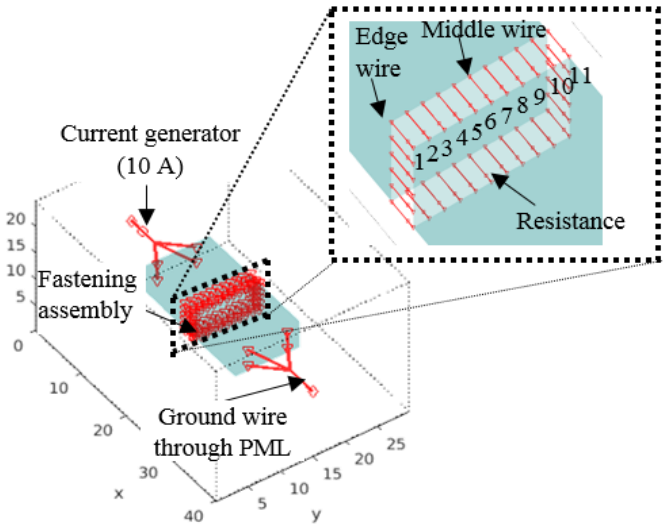

Fig. 10. 3D FDTD modelling of the fuel tank and a zoom on the fastening assembly. The axes are in number of cell involving a solution space size of 40x30x25 cells with a mesh size of 5 cm.

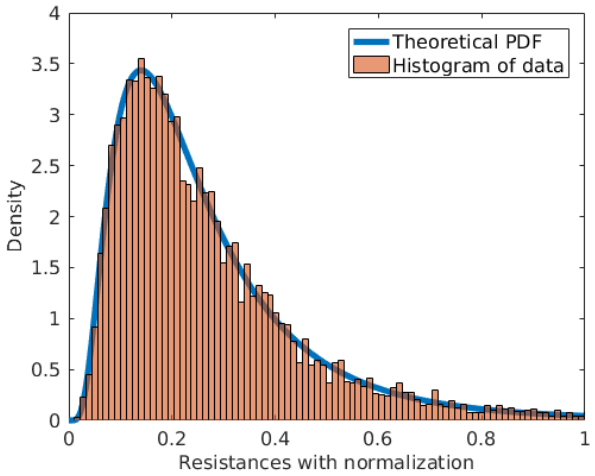

Fig. 11. Probability density histogram of computed data and lognormal theoretical PDF.

disturb the current or magnetic field behavior provided that:

$$\frac{\sigma}{\alpha^2 \varepsilon_0 \varepsilon_r \omega} >> 1, \tag{9}$$

$$\Delta < \frac{\lambda_{\min}}{10\alpha}, \tag{10}$$

$$f_{\max} < \frac{f_1^{res}}{\alpha}, \tag{11}$$

with, σ the lowest conductivity of conductive elements of the structure and f_1^{res} the first resonance frequency of the structure.

For all simulations, the FDTD cubic mesh size is 5 cm in each direction, the wires for feeding and return path have a radius of 1 mm and the radius of fastener wires is 1.67 cm. Adding wires in order to represent fasteners introduce some holes. It modifies the inductance and the E-field. As a consequence, the fasteners wires radius have been chosen in order to generate an equivalent inductance close to an equivalent plate. From our experience, the radius size has to be around 1/3 of the mesh size. The other wires are connected to the perfectly matched layers [46]. We search to evaluate the EM effects of each material for the same set-up of fasteners. Hence, two fuel tanks are studied in this paper, a perfect conductor one and a composite one with a 10000 $S.m^{-1}$ conductivity using low frequency thin-plate-model [47-49]. This kind of fastener modelling and the FDTD simulation method have been still validated in [50], [51] against measurement.

B. Statistical implementation

In section II, the fuel tank modelling has been described. Using the statistical results from section III, the fastening assembly model for the FDTD method may extended to take into account fastener uncertainties. Indeed, the resistance of each fastener can follow a statistical law. We choose to study a fuel tank after a supposed lightning strike using the lognormal distribution law established in section III.

As a reminder, a composite and a metallic fuel tank are compared. Even if the lognormal distribution law was established from metallic sample measurement, we apply it for the composite fuel tank modelling. We assume this choice although the resistances values are slightly different in both cases. Indeed, we want to define the effect of each material (composite and metallic) for an equivalent resistance distribution.

In order to have a good representation of each case, 250 FDTD simulations for each fuel tank are performed. For each simulation, the 30 random sets of resistance follow the lognormal distribution. The random draw is performed from the lognormal CDF:

$$F(x,\mu,\sigma) = \frac{1}{2}\left[erf\left(\frac{\ln(x)-\mu}{\sigma\sqrt{2}} \right) + 1 \right]. \tag{12}$$

In (12), x is the resistance value. Therefore, writing $x = f(y)$ with $y \sim U(0,1)$, gives:

$$x = exp\left(\sigma\sqrt{2} erf^{-1}(2y-1) + \mu \right). \tag{13}$$

Using (13) with $\mu = -1.524$ and $\sigma = 0.665$ for each set of resistance and each simulation we obtain 7380 samples (30 resistances x 246 simulations) following $logN(-1.524, 0.665)$. Fig. 11 presents the density probability histogram of our computed data and the theoretical lognormal PDF. The high number of simulations requires the use of the CALI supercomputer of University of Limoges.

C. Current distributions

In order to simplify the current distribution understanding, only the results in the edge wire and middle wire of the top fastening assembly are shown (see Fig. 10). Fig. 12 and Fig. 13 present the current distributions for each simulation from 100 Hz to 1 MHz in the composite and metallic fuel tank. Grey curves show the results of each simulation with a specific random set of fasteners resistances values, while the black curve with cross gives the results for a simulation where all the resistances have the same value which is the mean value of computed data (here 27.4 mΩ). The black curve with circle is the mean curve of grey ones.

Clearly, the current dispersion is stronger in a metallic fuel tank than in a composite one. The higher current is stronger in the metallic tank about 15 dB. As a result, the resistive effect of the composite has a major role in the current distribution limiting the impact of the fastener resistances. At “high” frequency, as for 500 kHz, the current distribution is the same whatever the kind of fuel tank because the resistive effect is overcome by the inductive effect. Obviously, the mean curves converge to the same values at low frequency whatever the fuel tank and the fastener are, as the current distribution becomes uniform. Moreover, the current increases with frequency in the edge wire and decreases in the middle wire according to the Lorentz force. Furthermore, throughout the frequency band, both black curves are similar. It should be equal for the metallic fuel tank, but it is not the case at low frequency. It might be explained by a local convergence issue for several simulations in the FDTD method due to small resistances values. Another explanation is the insufficient number of simulations considering the strong dispersion.

To conclude, the differences between the current distributions of the composite and metallic fuel tank concern extreme values, dispersion and cutoff-frequency.

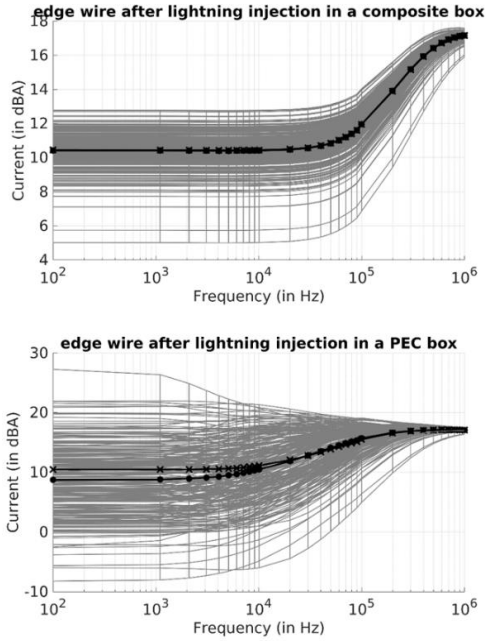

Fig. 12. Current distributions on the edge wire as a function of frequency for composite (top plot) and metallic (bottom plot) fuel tank with a lognormal distribution of fasteners resistances.

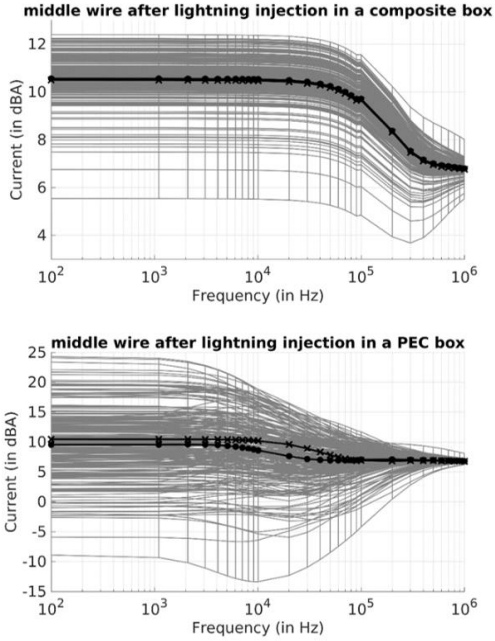

Fig. 13. Current distributions on the middle wire as a function of frequency for composite (top plot) and metallic (bottom plot) fuel tank with a lognormal distribution of fasteners resistances.

IV. Conclusion

A complete nonparametric statistical fitting method from measurement database has been proposed. This method lies on the use of the MLE method and several statistical tests and/or statistical criteria. It can be applied even for small samples issues but it requires continuous and independent data which constitute a unimodal distribution. If the unimodality is not respected, we propose a grouping method from physical hypothesis and statistical techniques in order to split the database in several unimodal populations. These statistical methods have been used in order to define the lightning injection electric effects on fastener resistances in an airplane fastening assembly. Moreover, the fastener resistances state after lightning injection has been studied from a statistical point of view. A lognormal law has been found as the better theoretical law characterizing this state. Then, this result has been used to supplement a simple electric fastener model. A study about the fastening assembly on a metallic fuel tank and a composite one has been carried out to quantify the current distributions. It aims to overcome fastener uncertainties and to estimate extreme values of current. Our simple fastener model seems to be really efficient and allows a representation of each kind of fasteners whatever their position. Nevertheless, some questions have to be raised about the introduction of holes in confined environments as fuel tanks involving local E-field disturbances. Future researches will be dedicated to investigate these questions and to improve our model. Moreover, it is planned to study this fastener model in a FDTD modelling of a realistic fuel tank.

References

[1] F. A. Fisher, J. A. Plumer, R.A. Perala, "*Lightning protection of aircraft*," 2nd edition. Lightning technologies Inc., 2004.

[2] D. Morgan, C.J. Hardwick, S.J. Haigh, A.J. Meakins, "The Interaction of Lightning with Aircraft and the Challenges of Lightning Testing," *Aerospace Lab*, pp. 1-10, 2012.

[3] EUROCAE Document ED-91. – Aircraft lightning zoning standard. Amendment 2, 2006.

[4] H. Mulazimoglu, L. Haylock, "Recent Developments in Techniques to Minimize Lightning Current Arcing Between Fasteners and Composites Structure," in *Proc. ICOLSE*, Oxford, UK, 2011.

[5] I. Revel, A. Herve, G. Peres, M. Webster, R. Maddison, F. Flourens, "Undestanding of edge glow phenomenon," in *Proc. ICOLSE*, Seattle (WA), 2013.

[6] L. Chemartin, P. Lalande, B. Peyrou, A. Chazottes, P.Q. Elias, C. Delalondre, B.G. Cheron, F. Lago, "Direct Effects of Lightning on Aircraft Structure: Analysis of the Thermal, Electrical and Mechanical Constraints," *AerospaceLab*, Issue 5, 2012.

[7] L. Chemartin, P. Lalande, F. Tristant, "Modeling and simulation of sparking in fastening assemblies," in *Proc. ICOLSE*, Seattle (WA), pp. 18-20, 2013.

[8] P. Teulet, T. Billoux, Y. Cressault, A. Gleizes, I. Revel, B. Lepetit, G. Peres, "Calculation of the pressure build-up around a fastener due to sparking," in *Proc. ICOLSE*, Oxford, UK, 2011.

[9] I. Revel, S. Evans, F. Flourens, "Edge glow: a combined voltage/power controlled mechanism? ," *ICLP, Estoril, Portugal*, 2016.

[10] J.A Plumer, J.D Robb, "The direct effects of lightning on aircraft," *IEEE Trans. Electromagn. Compat.*, vol. EMC-24, no. 2, pp. 158–172, 1982.

[11] L. Huang, C. Gao, F. Guo, C. Sun, "Lightning Indirect Effects on Helicopter: Numerical Simulation and Experimental Validation," *IEEE Trans. Electromagn. Compat.*, vol. 59, no. 4, pp. 1171 - 1179, 2017.

[12] M. Aprà, M. D'Amore, K. Gigliotti, M. S. Sarto, V. Volpi, "Lightning indirect effect certification of a transport aircraft by numerical simulation," *IEEE Trans. Electromagn. Compat*., vol. 50, no. 3, pp. 513–523,Aug. 2008.

[13] E. Perrin, C. Guiffaut, A. Reineix, and F. Tristant, "Using a design-of-experiment technique to consider the wire harness load impedances in the FDTD model of an aircraft struck by lightning," *IEEE Trans. Electromagn.Compat*., vol. 55, no. 4, pp. 747–753, Aug. 2013.

[14] M. S. Sarto, "Innovative absorbing boundary conditions for the efficient FDTD analysis of lightning interaction problems," *IEEE Trans. Electromagn.Compat*., vol. 43, no. 3, pp. 368–381, Aug. 2001.

[15] B.J.C. Burrows, "Scientific aspects of prevention of lightning induced sparks, fire, and explosion in above ground steel petroleum storage tank," in *Proc. ICOLSE*, Paris, France, 2007.

[16] S.J. Evans, "Fasteners: addressing the problem of sparking composite joints," *IET Lightning Protection for Aircraft Components Seminar, Abingdon, UK*, 2013.

[17] J. A. Plumer, L. C. Hoots, "Lightning protection with segmented diverters," in *Proc. Int. Symp. on Electromag. Compat.*, June 20-22, 1978, IEEE document 78-CH-1304-5 (EMC).
[18] B. Lepetit, I. Revel, G. Peres, L. Andrivet, F. Flourens, "In-strike dynamical measurements of contact resistances," in *Proc. ICLP*, Cagliari, Italy, 2010.
[19] J.H. Covey, "Arc suppression around fasteners", *Patent No. US4905931*, 2 Jan. 1990.
[20] R. Ranjith, R. S. Myong, "Computational simulation of lightning strike effects on aircraft fuel tank," in *Proc. ICOLSE*, Seattle (WA), 2013.
[21] A. Liebscher, H. Mulazimoglu, J-P. Moreau, W. Prachumsri, "Diagnostic technique for measuring contact resistivity at fastener-structure interfaces under static and flight load conditions," in *Proc. ICOLSE*, Nagoya, Japan, 2017.
[22] F. Fustin, F. Tristant, J.-P. Moreau, and F. Terrade, "Fuel tank safety – 3D distributions on fasteners/assemblies outside and inside fuel tanks," in *Proc. ICOLSE*, Seattle (WA), 2013.
[23] J. A. Hartigan, P. M. Hartigan, "The dip test of unimodality," *The annals of statistics*, vol. 13, No. 1, pp. 70–84, 1985.
[24] A. Cullen, H. Frey, *Probabilistic techniques in exposure assessment*. First Edition. Plenum Publishing Co, 1999.
[25] B. Efron, R.J. Tibshirani, *An Introduction to the Bootstrap.* First edition. Chapman & Hall, 1994.
[26] J. Aldrich, "R.A. Fisher and the making of maximum likelihood," *Statistical* Science, Vol. 12, No 3, 1997, pp. 162–176, 1922.
[27] H. Akaike, "Information theory and an extension of the maximum likelihood principle," *Second International Symposium on Information Theory*, p. 267-281, 1973.
[28] C. Lemoine, P. Besnier, M. Drissi, "Investigation of reverberation chamber measurements through high-power goodness-of-fit tests," *IEEE Trans. Electromagn. Compat.*, vol. 49, no. 4, pp. 745–755, Nov. 2007.
[29] M. H. Gail, S. B. Green, "Critical Values for the One-Sided Two-Sample Kolmogorov-Smirnov Statistic," *Journal of the American Statistical Association*, vol. 71, p.355, 1976.
[30] P.J. Kim, R.I. Jennrich, "Tables of the exact sampling distribution of the two sample Kolmogorov-Smirnov criterion $D_{mn}(m < n)$ ", in H.L. Harter and D.B. Owen (Eds.), *Selected Tables in Mathematical Statistics*, vol. I, Providence, RI: American Mathematical Society, 1973.
[31] X. Chen, "Using Akaike Information Criterion for Selecting the Field Distribution in a Reverberation Chamber," *IEEE Trans. Electromagn. Compat.*, vol. 55, no. 4, pp. 664–670, 2013.
[32] *Time ElectroMagnetic Simulator – Finite Difference software*, TEMSI-FD, CNRS, Univ. of Limoges, Limoges, France, 2006.
[33] F. Tristant, J-P Moreau, F. Fustin, F. Terrade, "Fuel tank safety – Methodology and assessment at structure level," in *Proc. ICOLSE, Seattle (WA)*, 2013.
[34] OM16 milliohmmeter / microhmmeter Datasheet, [Online]. Available: http://www.aoip.fr/product/micro-ohmmetres/om-16/. AOIP, BP 182, 91133 RIS ORANGIS CEDEX France
[35] L. Engelman, J. A. Hartigan, "Percentage points of a test for clusters," *Journal of the American Statistical Association*, vol. 64, no 328, p. 1647–1648, 1969.
[36] J. H. Wolfe, "Pattern clustering by multivariate mixture analysis," *Multivariate Behavioral Research*, vol. 5, no 3, p. 329–350, 1970.
[37] M. Hollander, D. A. Wolfe, *Nonparametric Statistical Methods*. John Wiley & Sons, New York-Sydney-Tokyo-Mexico City 1973.
[38] F. Wilcoxon, "Individual comparisons by ranking methods," *Biometrics bulletin*, vol. 1, no 6, p. 80–83, 1945.
[39] D. Vose, *Quantitative Risk Analysis. A Guide to Monte Carlo Simulation Modelling.* First edition. John Wiley & Sons, 2010.
[40] A. Luceño, "*Fitting the generalized Pareto distribution to data using maximum goodness-of-fit estimators*," *Computational Statistics & Data Analysis*, vol. 51, no. 2, pp. 904–917, 2006.
[41] M.A. Stephens, "Tests Based on EDF Statistics", in *Goodness-of-Fit Techniques*, ed. R. B. d'Agostino and M. A. I. N. Stephens, New York: Marcel Dekker, pp. 97–193, 1986.
[42] C. Guiffaut, A. Reineix, B. Pecqueux, "New Oblique Thin Wire Formalism in the FDTD Method With Multiwire Junctions," *IEEE Trans. Antennas Propag.*, vol. 60, no. 3, pp. 1458–1466, 2012.
[43] A. Jazzar, E. Clavel, G. Meunier, and E. Vialardi, "Study of lightning effects on aircraft with predominately composite structures," *IEEE Trans. Electromagn. Compat.*, vol. 56, no. 3, pp. 675–682, Jun. 2014.
[44] R.Holland, "Finite-difference time-domain(FDTD) analysis of magnetic Diffusion," *IEEE Trans. Electromagn. Compat.*, vol. 36, pp. 32–39, Nov. 1994.
[45] A.Taflove and S. C. Hagness, *Comput. Electrodynamics: The Finite-Difference Time-Domain Method*. 3rd ed. Boston, MA, USA, Artech House, 2005.
[46] J.-P. Bérenger, "Perfectly matched layer for the FDTD solution of wave-structure interaction problems," *IEEE Trans. Atennas Propag.*, vol. 44, no. 1, pp. 110–117, 1996.
[47] J.-P. Bérenger, "Plaques minces aux différences finies," in *Proc. Colloq. Int. Expo. Compat. Electromagn. (CEM)*, Lyon, France, 1992, pp. 298–303.
[48] R. J. Luebbers and K. Kunz, "FDTD modeling of thin impedance sheets," *IEEE Trans. Antennas Propag.*, vol. 40, pp. 349–351, Mar. 1992.
[49] C. J. Railton and J. P. McGeehan, "An analysis of microstrip with rectangular and trapezoidal conductor cross sections," *IEEE Trans. Microwave Theory Tech.*, vol. 38, pp. 1017–1022, Aug. 1990.
[50] F. Tristant, F. Fustin, F. Terrade, M. Roussel, F. Parfait, F. Lago, M. Berthet, A. Laisné, C. Guiffaut, and A. Reineix, "Fuel tank safety – 3D computations for attachment and conduction assessment," in *Proc. ICOLSE*, Toulouse, France, Sep. 2015.
[51] P. Monferran, C. Guiffaut, A. Reineix, F. Fustirr, and F. Tristant, "Fastening assemblies modelling in finite difference time domain," in *Proc. Int. Symp. Electromagn. Compat. (EMC EUROPE)*, Aug 2018, pp. 521–526.

Biographies of the other co-authors are currently not available.